



## Production rates of cosmogenic helium-3, neon-21, and neon-22 in ordinary chondrites and the lunar surface

J. MASARIK<sup>1†</sup>, K. NISHIIZUMI<sup>1\*</sup> AND R. C. REEDY<sup>2</sup>

<sup>1</sup>Space Sciences Laboratory, University of California, Berkeley, California 94720-7450, USA

<sup>2</sup>Space and Remote Sensing Sciences Group, MS-D436, Los Alamos National Laboratory, Los Alamos, New Mexico 87545, USA

<sup>†</sup>Present address: Department of Nuclear Physics, Komensky University, Mlynska dolina F/1, Sk-842 15 Bratislava, Slovakia

\*Correspondence author's e-mail address: [kuni@ssl.berkeley.edu](mailto:kuni@ssl.berkeley.edu)

(Received 2000 November 17; accepted in revised form 2001 January 26)

**Abstract**—The production of <sup>3</sup>He, <sup>21</sup>Ne, and <sup>22</sup>Ne in meteoroids of various sizes and in the lunar surface was investigated. The LAHET code system, a purely physical model for calculating cosmic-ray particle fluxes, was used to simulate cosmic-ray particle interactions with extraterrestrial matter. We discuss the depth and size dependence of the shielding parameter <sup>22</sup>Ne/<sup>21</sup>Ne, which is used for reconstruction of pre-atmospheric sizes, depth, and exposure histories. The <sup>22</sup>Ne/<sup>21</sup>Ne ratio decreases with increasing depth or pre-atmospheric size but then increases with depth in very large objects. This increase with depth in the <sup>22</sup>Ne/<sup>21</sup>Ne ratio means that this ratio is a poor indicator of shielding in some large objects. The dependence of <sup>3</sup>He/<sup>21</sup>Ne as function of <sup>22</sup>Ne/<sup>21</sup>Ne was also calculated, and differences between the calculations and the Bern line are discussed.

### INTRODUCTION

The interactions of cosmic-ray particles with extraterrestrial materials produce a cascade of secondary particles and a variety of cosmogenic nuclides. These cosmogenic nuclides have a wide range of applications in dating and tracing various events in the history of the investigated object. They provide information about exposure ages, exposure history (simple or complex), terrestrial ages, pre-atmospheric size and shielding conditions of samples, as well as about the history of the cosmic radiation itself. For all applications, it is extremely important to know the production rates as a function of depth in objects of various radii and chemical compositions. The isotopes <sup>3</sup>He, <sup>21</sup>Ne, and <sup>22</sup>Ne and their ratios are very often used to study cosmic-ray exposure records so, in this paper, we consider their cosmogenic production.

A variety of models exists for the calculation of cosmogenic-nuclide production rates in extraterrestrial matter (see, e.g., Bhandari *et al.*, 1993; Graf *et al.*, 1990a; Honda, 1988; Leya *et al.*, 2000; Masarik *et al.*, 1992; Masarik and Reedy, 1994b; Michel *et al.*, 1991, 1996; Reedy, 1985, 1987; Reedy and Arnold, 1972). The majority of the models, especially those developed before about 1990, use approximations with a very limited set of parameters. Since 1990, better models for calculating production rates of cosmogenic nuclides have been developed. Most of these newer models use only basic physical quantities and principles, without including any free parameters, to simulate numerically all processes relevant in particle production and transport. As

such models enable us to follow the history of individual cosmic-ray particles, we are able to determine the main sources of observed production rate dependencies. One also can do calculations for any composition and exposure geometry.

To estimate the shielding conditions, the <sup>22</sup>Ne/<sup>21</sup>Ne ratio for stony meteorites is widely used. Production rates for many cosmogenic nuclides in ordinary chondrites are usually determined as a function of the <sup>22</sup>Ne/<sup>21</sup>Ne ratio (e.g., Eugster, 1988; Nishiizumi *et al.*, 1980). However, the <sup>22</sup>Ne/<sup>21</sup>Ne ratio is usually not used below values of about 1.08 as this ratio changes little with increased shielding. This ratio is usually assumed to become constant at about 1.06 for ordinary chondrites when the shielding gets large, that is, deep inside large objects (e.g., Jentsch and Schultz, 1996). However, the behavior of the <sup>22</sup>Ne/<sup>21</sup>Ne ratio in very large objects has not been well studied to confirm that this ratio remains a constant.

The Jilin H5 chondrite was a large object when it fell and had an earlier exposure as a nearly  $2\pi$  object. The isotopes of the light noble gases have been measured in many samples of Jilin (e.g., Begemann *et al.*, 1996). A plot of the <sup>22</sup>Ne/<sup>21</sup>Ne ratio as a function of the <sup>21</sup>Ne concentration for samples of Jilin shows that the <sup>22</sup>Ne/<sup>21</sup>Ne ratio for the lowest values of the <sup>21</sup>Ne concentration increases relative to samples with intermediate <sup>21</sup>Ne concentrations (Jentsch and Schultz, 1996). Some of the increase (from 1.06 to about 1.075) is probably caused by Jilin's complex exposure history, as shown by samples from core B, which was drilled parallel to the surface exposed during Jilin's first cosmic-ray exposure, and by other samples from the main mass. The samples with the lowest

concentrations of  $^{21}\text{Ne}$  had  $^{22}\text{Ne}/^{21}\text{Ne}$  ratios up to 1.09, suggesting that the  $^{22}\text{Ne}/^{21}\text{Ne}$  ratio increases with large amounts of shielding. The Gold Basin L4 chondrite was a very large object in space with a possible complex exposure history (Welten *et al.*, 2001; Wieler *et al.*, 2000). In specimens of Gold Basin, the  $^{22}\text{Ne}/^{21}\text{Ne}$  ratio first decreases then increases as a function of decreasing  $^{21}\text{Ne}$  concentrations (Wieler *et al.*, 2000).

A plot of the  $^3\text{He}/^{21}\text{Ne}$  ratio as a function of the  $^{22}\text{Ne}/^{21}\text{Ne}$  ratio is often used for shielding corrections and to test for possible losses of cosmogenic  $^3\text{He}$ . The relation between these two ratios is usually assumed to be a straight line, called the "Bern Line" (Eberhardt *et al.*, 1966). Data for  $^3\text{He}/^{21}\text{Ne}$  as a function of  $^{22}\text{Ne}/^{21}\text{Ne}$  in samples of various meteorites generally follow this trend, although the slope of this line for several samples from an individual meteorite is usually a little less than the trend line, although they cluster around the line (e.g., Graf *et al.*, 1990a; Jentsch and Schultz, 1996; Nishiizumi *et al.*, 1980). Samples with heavy shielding are traditionally believed to cluster at the end of this line with the lowest ratios (about 1.06 for  $^{22}\text{Ne}/^{21}\text{Ne}$  and 3.5 for  $^3\text{He}/^{21}\text{Ne}$ ). Samples that plot below this line are assumed to have lost some of their cosmogenic  $^3\text{He}$ .

For the case of a simple cosmic-ray exposure history, the meteoroid was exposed to cosmic rays only after ejection from a heavily-shielded location in its parent body. Cosmogenic nuclide records in the majority of chondrites indicate such simple exposure histories (e.g., Eugster, 1988). However,

comparisons of the concentrations of cosmogenic radionuclides and noble gases indicate that some meteoroids were exposed to cosmic rays both near the surface of its parent body and, after ejection, in space as a small body (e.g., Nishiizumi *et al.*, 1979). Wetherill (1980, 1985) predicted that complex, or multi-stage, exposure histories should be common among chondrites. It is now recognized that planetary perturbations (e.g., orbital resonances such as the 3:1 one with Jupiter) and the Yarkovsky thermal forces can modify meteoroid orbits and deliver meteorites to the Earth, although many numerical simulations of such processes still include collisional events. The model of Vokrouhlicky and Farinella (2000) has collisions occurring on time scales of a few million years, and these authors note that complex exposure histories "should be commonplace". However, we only have a short list of meteorites that have evidences of complex exposure histories (e.g., Herzog *et al.*, 1997; Heusser *et al.*, 1985; Nishiizumi *et al.*, 1979). We have noticed that some meteorites with complex-exposure histories have  $^{22}\text{Ne}/^{21}\text{Ne}$  ratios higher than about 1.08, even though most of the cosmic-ray exposure occurred in a large body.

Figure 1 shows  $^3\text{He}/^{21}\text{Ne}$  vs.  $^{22}\text{Ne}/^{21}\text{Ne}$  in H and L chondrites. We calculated these ratios from data published after 1971 that were taken from the compilations of L. Schultz (Schultz and Kruse, 1989, and supplement by Schultz and Franke, pers. comm., 2000). Averages were used for multiple measurements in one meteorite. The "Bern Line" (Eberhardt *et al.*, 1966) is also shown in the figure. In this paper, we adopted the relation of the "Bern Line" from Nishiizumi *et al.*

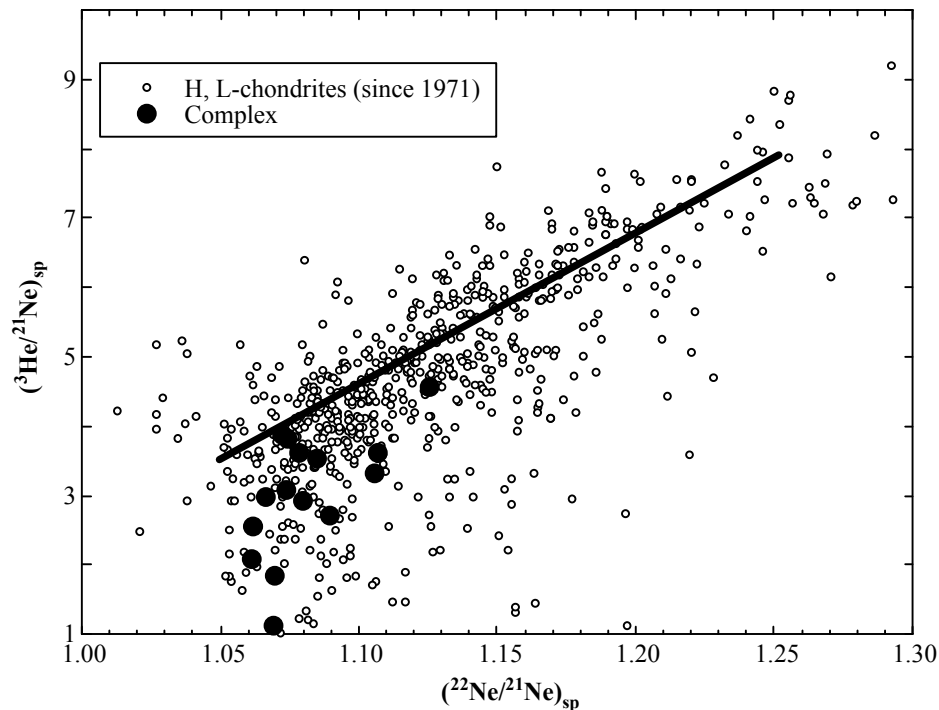


FIG. 1. The cosmogenic  $^3\text{He}/^{21}\text{Ne}$  vs.  $^{22}\text{Ne}/^{21}\text{Ne}$  measured for samples of H and L chondrites and for chondrites with complex exposure histories (filled circles).

(1980). When the  $^3\text{He}/^{21}\text{Ne}$  and  $^{22}\text{Ne}/^{21}\text{Ne}$  ratios from meteorites with complex exposure histories are plotted (filled circles in Fig. 1), they tend to fall below the Bern Line. Such samples have traditionally been assumed to have lost some of their cosmogenic  $^3\text{He}$ . However, if as suggested above using data from Jilin and Gold Basin that the  $^{22}\text{Ne}/^{21}\text{Ne}$  ratio increases with heavy shielding, then some of the meteorites with complex histories that fall below the trend line might not have lost  $^3\text{He}$  but fall below the line because of a higher  $^{22}\text{Ne}/^{21}\text{Ne}$  ratio.

In this paper, we use the LAHET code system (LCS) to investigate the production systematics for  $^3\text{He}$  and neon isotopes in large stony meteorites. The cosmogenic  $^{22}\text{Ne}/^{21}\text{Ne}$  and  $^3\text{He}/^{21}\text{Ne}$  ratios are also investigated. As the production rates and ratios of these isotopes in lunar samples are often derived using old models, such as Hohenberg *et al.* (1978) using the model of Reedy and Arnold (1972), we did calculations for a range of depths in the Moon.

### CALCULATIONAL MODEL

Our model for the numerical simulation of the primary and secondary cosmic-ray particles is LCS (Masarik and Reedy, 1994b). LCS combines the Los Alamos high-energy transport (LAHET) code (Prael and Lichtenstein, 1989) for interactions of charged particles and neutrons above 20 MeV and the Monte Carlo N-Particle (MCNP) code (Briesmeister, 1993) for low-energy neutrons. These codes use Monte Carlo calculations to treat the relevant physical processes of particle production and transport.

Our use of LCS-calculated particles fluxes and evaluated cross sections for determined cosmogenic-nuclide production rates has been tested for the radionuclide production profiles in many meteorites, such as Knyahinya (Reedy *et al.*, 1993), St. Séverin (Masarik and Reedy, 1994a), Canyon Diablo (Michlovich *et al.*, 1994), and Norton County (Englert *et al.*, 1995). As this code system is described in detail elsewhere (Masarik and Reedy, 1994b), we repeat here only its main features.

Only primary galactic cosmic-ray (GCR) protons with energies between 10 MeV and 20 GeV were considered using a long-term-averaged solar modulation parameter (550 MeV). For the Moon, we used the effective flux of protons determined from lunar cosmogenic radionuclides of  $4.56 \text{ nucleons cm}^{-2} \text{ s}^{-1}$  for energies above 10 MeV (Reedy and Masarik, 1994). For H chondrites, we used the effective proton fluxes determined from radionuclides in Knyahinya of  $4.8 \text{ nucleons cm}^{-2} \text{ s}^{-1}$  for energies above 10 MeV (Reedy *et al.*, 1993).

For these calculations, the investigated objects were considered as spheres with various radii or semi-infinite slabs. The spheres were divided into spherical layers and the slabs were divided into parallel layers to account for variation of the particle fluxes with depth inside the irradiated object. The thicknesses of layers varied from 1 cm (for small meteoroids)

to 4 cm (for large meteorites and slabs). The elemental weight fractions and densities of the objects were taken from Wasson and Kallemeyn (1988) for H chondrites (Mg = 0.140, Al = 0.0113, Si = 0.169, Ca = 0.0125, and Fe = 0.275) and from Nishiizumi *et al.* (1984) for the lunar surface (Mg = 0.0643, Al = 0.071, Si = 0.219, Ca = 0.0739, and Fe = 0.120).

The production rate of a cosmogenic nuclide from a given element was obtained by integrating over energy the product of the LCS-calculated fluxes and cross sections for both protons and neutrons. Elemental values were summed to get the total production rate. The statistical errors of the flux calculations were at the level of 2–3%. For the cross sections for the production of  $^3\text{He}$ ,  $^{21}\text{Ne}$ , and  $^{22}\text{Ne}$ , we used literature values when available (*e.g.*, Reedy, 1992; Reedy *et al.*, 1979) or values evaluated by us and tested by earlier calculations for a wide range of objects and their sizes (*e.g.*, Hohenberg *et al.*, 1978; Masarik and Reedy, 1994a,b, 1995).

### THE DEPTH AND SIZE DEPENDENT HELIUM-3, NEON-21, AND NEON-22 PRODUCTION RATES AND CORRELATIONS AMONG THEM

For additional tests of our model calculations with experimental data, we used data for the light noble gases measured in Keyes (Wright *et al.*, 1973) and Knyahinya (Graf *et al.*, 1990b). Both meteorites were simulated as spherical objects with L-chondrite chemical composition and with radii of 30 and 45 cm, respectively. Within the experimental errors of ~5% the model reproduces the shapes of all depth profiles. Figures 2–4 show the comparison of measured and calculated production rates of  $^{21}\text{Ne}$ ,  $^3\text{He}$ , and the  $^{22}\text{Ne}/^{21}\text{Ne}$  production ratio in the Knyahinya meteorite for its exposure age of 39 Ma.

The production rates and ratios for  $^3\text{He}$ ,  $^{21}\text{Ne}$ , and  $^{22}\text{Ne}$  in larger objects were calculated. Figure 5 presents the  $^{22}\text{Ne}/^{21}\text{Ne}$  production ratio as a function of depth in the lunar surface calculated using LCS and the Reedy–Arnold model (Hohenberg *et al.*, 1978). We used the Apollo 15 long core chemical composition and the same cross sections for both calculations. The  $^{22}\text{Ne}/^{21}\text{Ne}$  GCR production ratios calculated for this core using the elemental production rates of Hohenberg *et al.* (1978) are lower than those in Fig. 5 by about 0.03 because those authors used earlier sets of cross sections than the sets used here. The main difference between the two models is the continuous decrease in the ratio according to the Reedy–Arnold model *vs.* a trend with the ratio calculated using LCS first decreasing, reaching a minimum, and then gradually increasing. This shows that simple models, like the Reedy–Arnold one with only a single parameter for the flux shape as a function of depth, are often limited in their ability to yield good results.

Similar trends for the  $^{22}\text{Ne}/^{21}\text{Ne}$  production ratios calculated by LCS were also obtained for large meteoroids with H-chondrite chemical compositions (Fig. 6). These ratios as a function of depth for the meteoroids with the radii ranging from 40 to 500 cm are presented in Fig. 6. Using the calculated

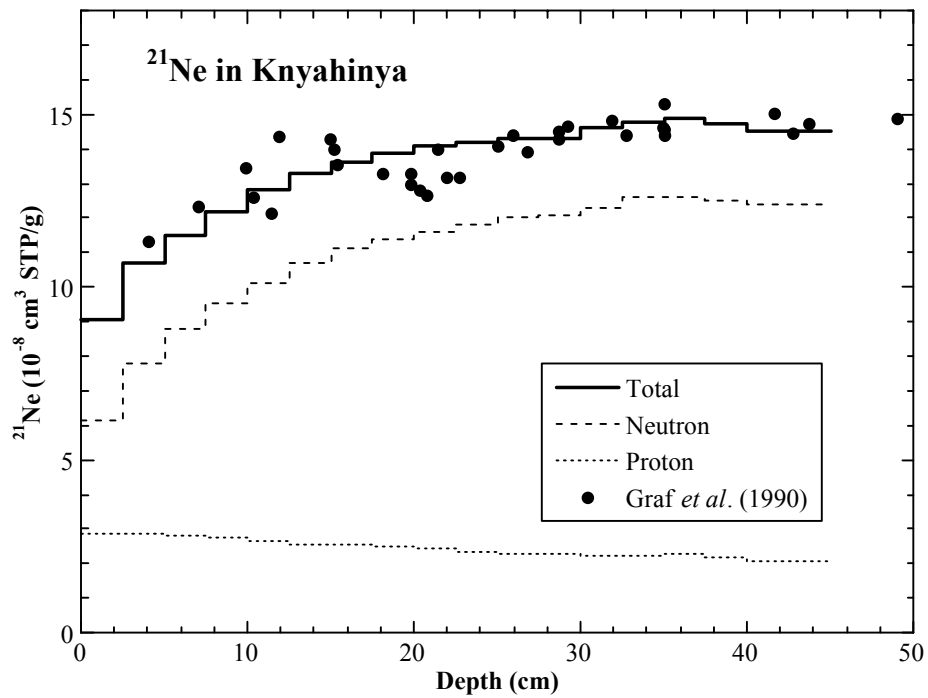


FIG. 2. Calculated depth profile (line) of  $^{21}\text{Ne}$  in Knyahinya. The experimental data (filled circles) are from Graf *et al.* (1990b).

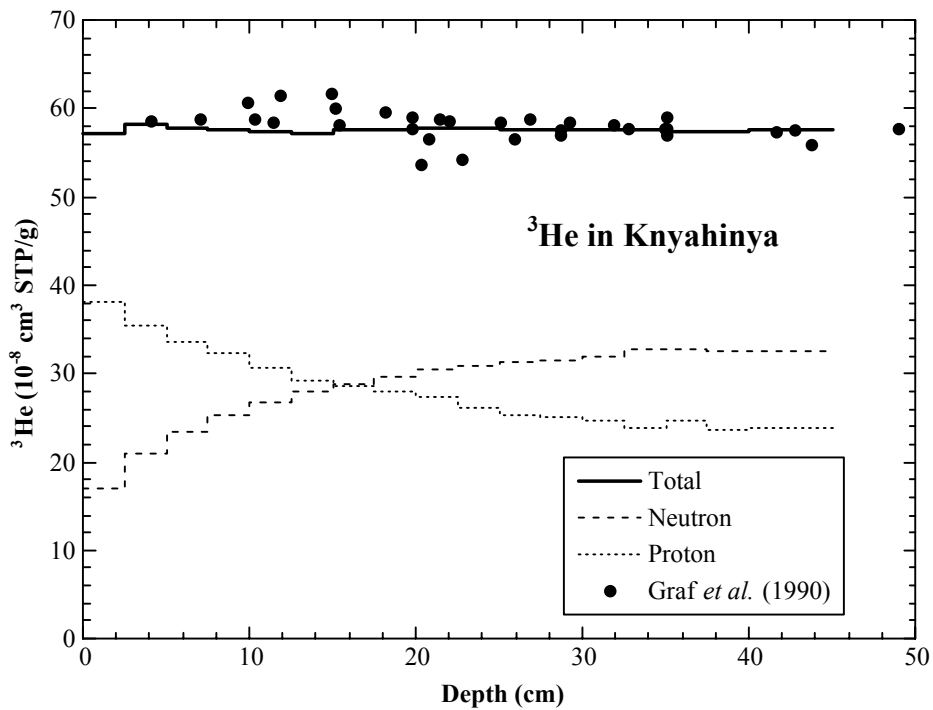


FIG. 3. Calculated depth profile (line) of  $^3\text{He}$  in Knyahinya. The experimental data (filled circles) are from Graf *et al.* (1990b).

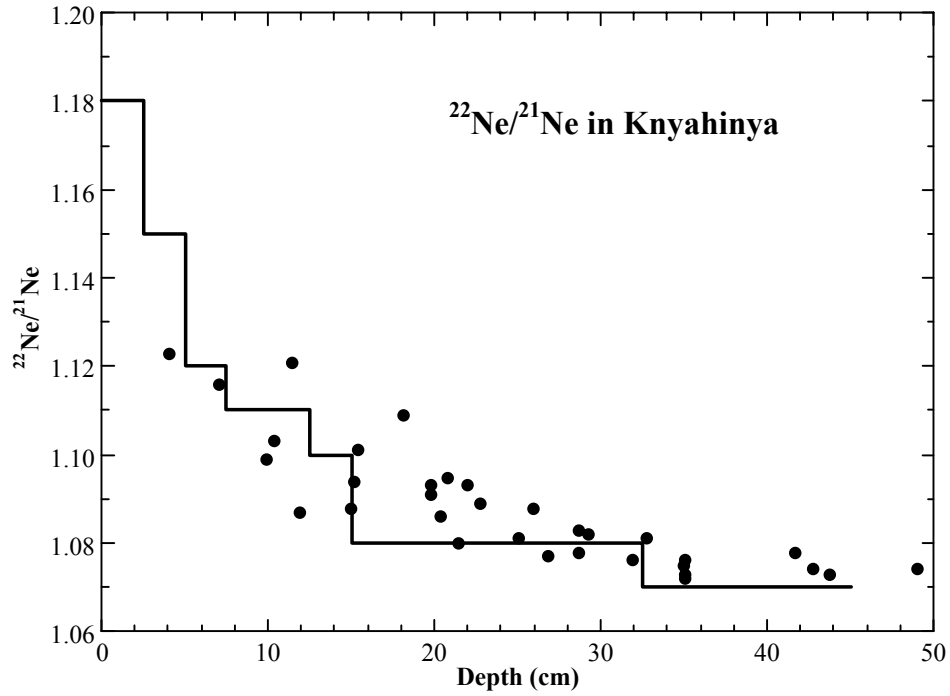


FIG. 4. Calculated depth profile (line) of the  $^{22}\text{Ne}/^{21}\text{Ne}$  ratio in Knyahinya. The experimental data (filled circles) are from Graf *et al.* (1990b).

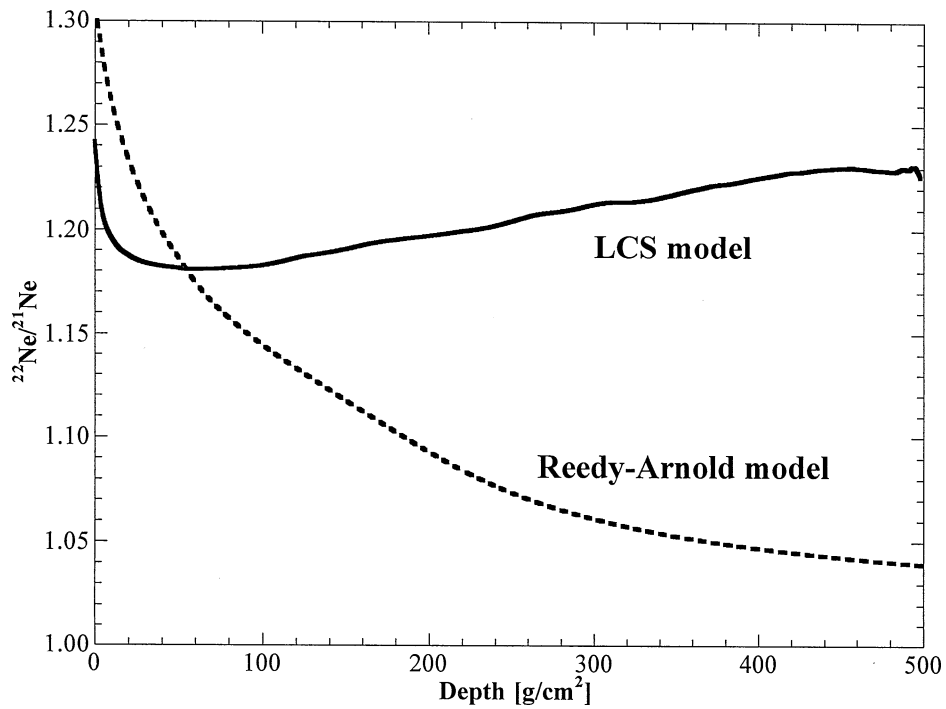


FIG. 5. Depth profile of the  $^{22}\text{Ne}/^{21}\text{Ne}$  ratio in the lunar surface calculated with the Reedy-Arnold model (dotted line) and with LCS (full line).

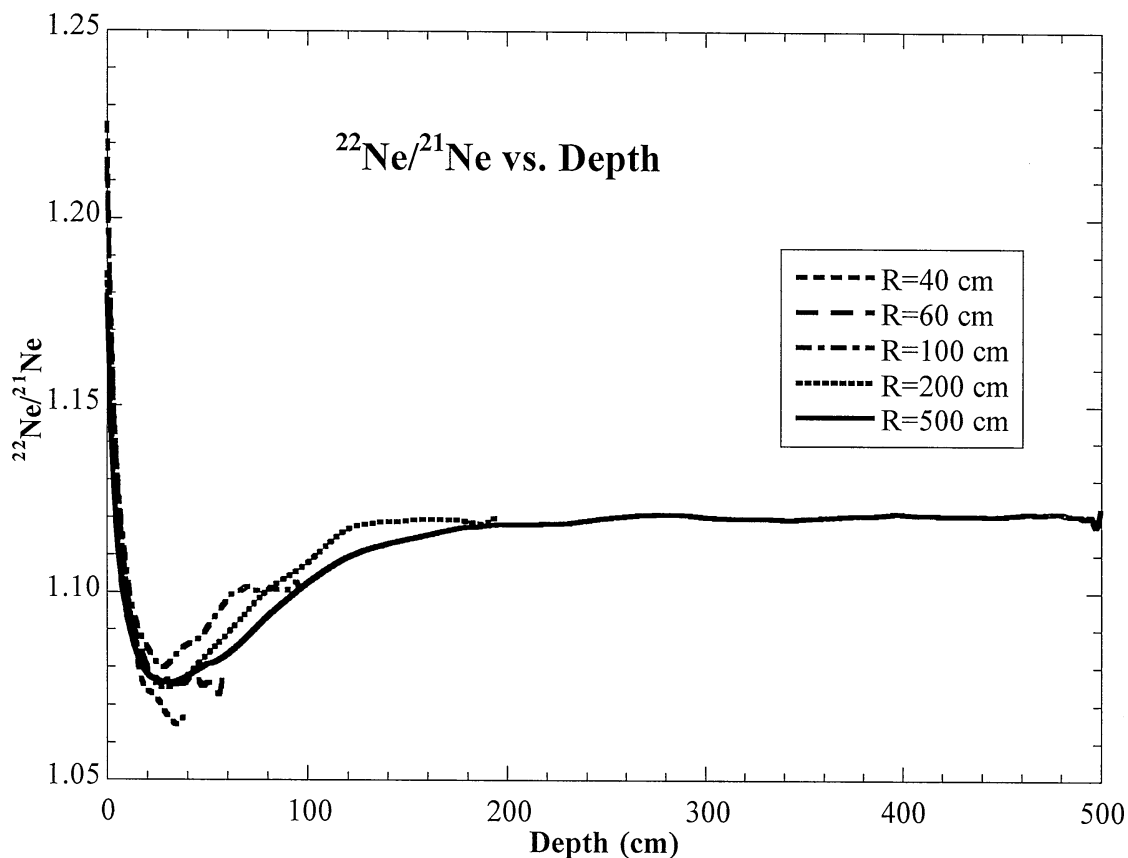


FIG. 6. Depth profile of the  $^{22}\text{Ne}/^{21}\text{Ne}$  ratio in H chondrites of various radii calculated with LCS.

production rates, the  $^3\text{He}/^{21}\text{Ne}$  ratio vs.  $^{22}\text{Ne}/^{21}\text{Ne}$  ratio in H chondrites were plotted (Fig. 7). The trend for the  $^3\text{He}/^{21}\text{Ne}$  ratio vs.  $^{22}\text{Ne}/^{21}\text{Ne}$  in the Moon is similar to that for very large chondrites.

This trend of the  $^{22}\text{Ne}/^{21}\text{Ne}$  ratio first decreasing and then eventually increasing with increasing depth is a consequence of the differences in the trend for the production of neon from magnesium compared to the trends for the other elements. Calculations done for the  $^{22}\text{Ne}/^{21}\text{Ne}$  ratio from Al, Si, Ca, and Fe in the Moon all have a similar trend below depths of  $\sim 10 \text{ g/cm}^2$  of slowly increasing monotonically with increasing depth, with their  $^{22}\text{Ne}/^{21}\text{Ne}$  ratios approaching constant values at depths below  $\sim 500 \text{ g/cm}^2$ . The calculated trend for the  $^{22}\text{Ne}/^{21}\text{Ne}$  ratio from Mg has a strong decrease from the surface to about  $100 \text{ g/cm}^2$  and a very slow increase for depths below about  $250 \text{ g/cm}^2$ . Thus, as noted by Reedy *et al.* (1979), magnesium controls the behavior of the  $^{22}\text{Ne}/^{21}\text{Ne}$  ratio.

Our calculations show that the production rates of cosmic-ray-produced noble gases depend on the size and shielding depth for very large objects in ways not previously predicted. As noted by Graf *et al.* (1990a), the  $^{22}\text{Ne}/^{21}\text{Ne}$  ratio is of limited use for objects larger than 30 cm and for small values of this ratio. We show for the first time that the trend for the  $^{22}\text{Ne}/^{21}\text{Ne}$  ratio linearly-correlating with  $^3\text{He}/^{21}\text{Ne}$  ratio does not work

for very large chondrites. Low values of  $^3\text{He}/^{21}\text{Ne}$  can be an indicator of complex exposure history.

The previous dependencies of shielding parameters were obtained from the analysis of experimental data from small chondrites (radii less than 45 cm). Also theoretical modeling was limited to a similar range of radii or, for larger objects, the depths below 50 cm were investigated as one or a very few large depth bins (in order to lower the statistical errors of the calculations), and therefore the variation of shielding parameters could not be investigated. Our calculations show that the  $^{22}\text{Ne}/^{21}\text{Ne}$  ratio at larger depths in meteorites and also in lunar surface do not show only a gradual decrease or constancy at depth. After reaching some minimal value (1.05–1.06), this ratio starts to increase (Figs. 6–7). Based on this depth dependence, we conclude that  $^{22}\text{Ne}/^{21}\text{Ne}$  ratio is not a good indicator of depth for objects with radii above 60 cm. Previously, it was assumed that the  $^{22}\text{Ne}/^{21}\text{Ne}$  ratio was not a good shielding indicator for  $^{22}\text{Ne}/^{21}\text{Ne}$  ratios below about 1.08. Our calculations show that the  $^{22}\text{Ne}/^{21}\text{Ne}$  ratio is not an unambiguous shielding indicator for  $^{22}\text{Ne}/^{21}\text{Ne}$  ratios below about 1.12. Interestingly, the completely different approach to the study of cosmogenic nuclide systematics of Honda (1988) also predicted an increasing  $^{22}\text{Ne}/^{21}\text{Ne}$  ratio in center of large objects (M. Honda, pers. comm., 1994).

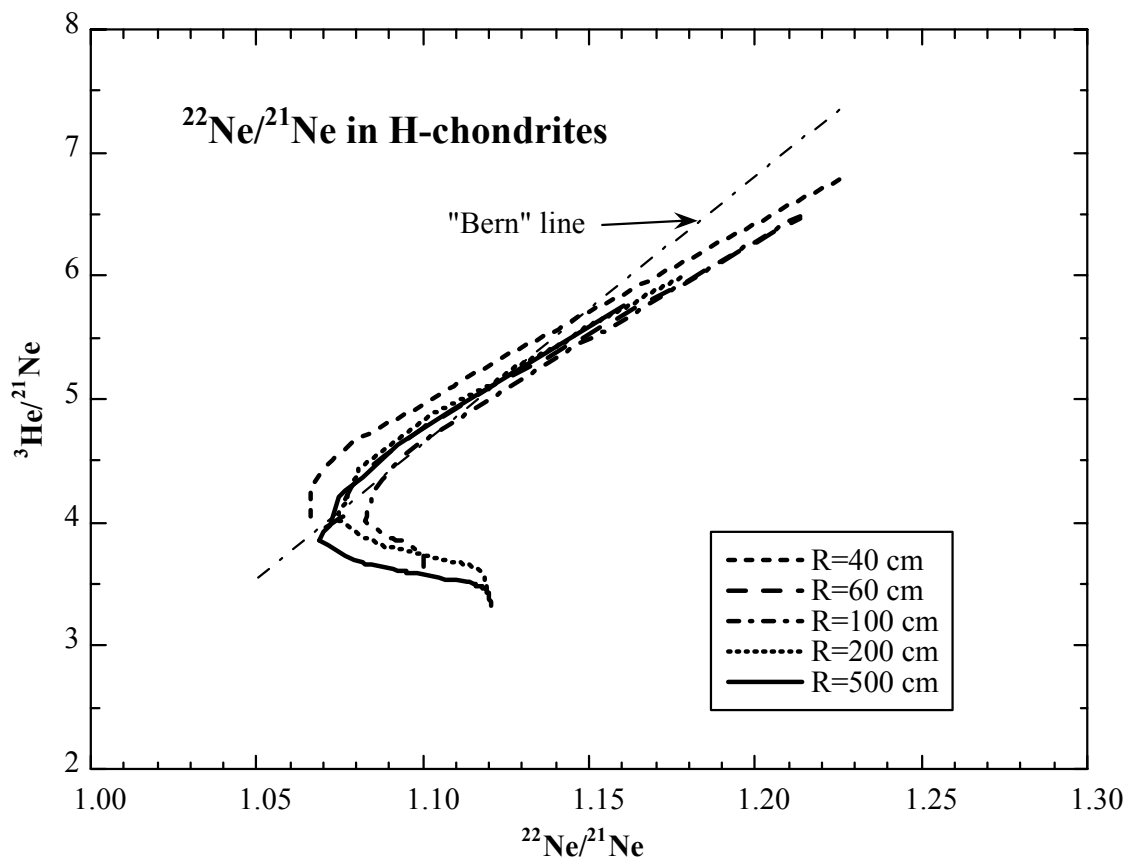


FIG. 7.  ${}^3\text{He}/{}^{21}\text{Ne}$  vs.  ${}^{22}\text{Ne}/{}^{21}\text{Ne}$  calculated for all pre-atmospheric depths in H chondrites of various radii and for the "Bern Line".

The complex dependence of the  ${}^{22}\text{Ne}/{}^{21}\text{Ne}$  ratio on depth inside a large irradiated object (with radii above 60 cm) leads to the nonlinear correlation between  ${}^3\text{He}/{}^{21}\text{Ne}$  and  ${}^{22}\text{Ne}/{}^{21}\text{Ne}$  (Fig. 7). The complex structure of the  ${}^3\text{He}/{}^{21}\text{Ne}$  dependence on  ${}^{22}\text{Ne}/{}^{21}\text{Ne}$  shows that not all meteorites for which  ${}^3\text{He}/{}^{21}\text{Ne}$  ratio falls below the Bern Line had to suffer  ${}^3\text{He}$  losses. However, our calculations do not predict  ${}^3\text{He}/{}^{21}\text{Ne}$  ratios less than about 3.5, so  ${}^3\text{He}/{}^{21}\text{Ne}$  ratios less than 3.5 are most likely due to the loss of  ${}^3\text{He}$ . The irradiation at deep locations inside a large object or complex exposure history in large objects can also lead to the  ${}^3\text{He}/{}^{21}\text{Ne}$  ratios lower than predicted by linear models. The observed data points of some of the complex-exposure meteorites in Fig. 1 could be on mixing lines between the end points for the meteorite's exposure in a large object and its latest exposure as a small meteoroid.

### SUMMARY AND CONCLUSIONS

We presented the results of  ${}^3\text{He}$ ,  ${}^{21}\text{Ne}$  and  ${}^{22}\text{Ne}$  production-rate calculations using numerical simulations done with the LAHET code system. The model calculations are based on well-tested data sets for nuclear cross sections. Particle fluxes were calculated with low statistical errors and with fine depth

bins, which was necessary for the study of fine structure of the depth-dependence production rates and their ratios. Our calculations showed that the  ${}^{22}\text{Ne}/{}^{21}\text{Ne}$  ratio in chondrites with radius above 60 cm and also in lunar surface reach a minimum at certain depths and then starts to increase at greater depths. This leads to a complex structure of the  ${}^3\text{He}/{}^{21}\text{Ne}$  ratio as a function of the  ${}^{22}\text{Ne}/{}^{21}\text{Ne}$  ratio. Based on these calculations, we can conclude that  ${}^{22}\text{Ne}/{}^{21}\text{Ne}$  is not a good indicator of depth for large chondrites and in the lunar surface. Caution thus is needed in using these ratios for meteorites with unknown pre-atmospheric sizes. It was also shown that the  ${}^3\text{He}/{}^{21}\text{Ne}$  ratio can be lower than predicted by Bern Line in large objects and need not be the indicator of  ${}^3\text{He}$  diffusion loss.

*Acknowledgements*—We wish to thank Dr. M. Honda for encouraging us for this line of study. We thank Drs. A. J. T. Jull and K. C. Welten for their thoughtful reviews of this paper. This work was supported by NASA grant NAG 5-4992 and DOE grant DE-FG03-96ER14676 at Berkeley and NASA work order W-19,620 at Los Alamos. The work at the Los Alamos National Laboratory was done under the auspices the U.S. Department of Energy by the University of California under contract No. W-7405-ENG-36.

*Editorial handling:* I. C. Lyon

## REFERENCES

- BEGEMANN F., CAIYUN F., WEBER H. W. AND XIANBIN W. (1996) Light noble gases in Jilin: More of the same and something new. *Meteorit. Planet. Sci.* **31**, 667–674.
- BHANDARI N. *ET AL.* (1993) Depth and size dependence of cosmogenic nuclide production rates in stony meteoroids. *Geochim. Cosmochim. Acta* **57**, 2361–2375.
- BRIESMEISTER J. F. (1993) *MCNP—A General Monte Carlo N-particle Transport Code, Version 4A*. Los Alamos National Laboratory Report **LA-12625-M**, Natl. Tech. Info. Service, Springfield, Virginia, USA. 693 pp.
- EBERHARDT P., EUGSTER O., GEISS J. AND MARTI K. (1966) Rare gas measurements in 30 stone meteorites. *Z. Naturforsch.* **21a**, 414–426.
- ENGLERT P. A. J., SARAFIN R., MASARIK J. AND REEDY R. C. (1995) Cosmogenic  $^{53}\text{Mn}$  in the main fragment of the Norton County aubrite. *Geochim. Cosmochim. Acta* **59**, 825–830.
- EUGSTER O. (1988) Cosmic-ray production rates for  $^3\text{He}$ ,  $^{21}\text{Ne}$ ,  $^{38}\text{Ar}$ ,  $^{83}\text{Kr}$ , and  $^{126}\text{Xe}$  in chondrites based on  $^{81}\text{Kr}$ -Kr exposure ages. *Geochim. Cosmochim. Acta* **52**, 1649–1662.
- GRAF T., BAUR H. AND SIGNER P. (1990a) A model for the production of cosmogenic nuclides in chondrites. *Geochim. Cosmochim. Acta* **54**, 2521–2534.
- GRAF T. *ET AL.* (1990b) Cosmogenic nuclides and nuclear tracks in the chondrite Knyahinya. *Geochim. Cosmochim. Acta* **54**, 2511–2520.
- HERZOG G. F., VOGT S., ALBRECHT A., XUE S., FINK D., KLEIN J., MIDDLETON R., WEBER H. W. AND SCHULTZ L. (1997) Complex exposure histories for meteorites with "short" exposure ages. *Meteorit. Planet. Sci.* **32**, 413–422.
- HEUSSER G., OUYANG Z., KIRSTEN T., HERPERS U. AND ENGLERT P. (1985) Conditions of the cosmic ray exposure of the Jilin chondrite. *Earth Planet. Sci. Lett.* **72**, 263–272.
- HOHENBERG C. M., MARTI K., PODOSEK F. A., REEDY R. C. AND SHIRCK J. R. (1978) Comparisons between observed and predicted cosmogenic noble gases in lunar samples. *Proc. Lunar Planet. Sci. Conf.* **9th**, 2311–2344.
- HONDA M. (1988) Statistical estimation of the production of cosmic-ray-induced nuclide in meteorites. *Meteoritics* **23**, 3–12.
- JENTSCH O. AND SCHULTZ L. (1996) Cosmogenic noble gases in silicate inclusions of iron meteorites: Effects of bulk composition on elemental production rates. *J. Royal Soc. West. Australia* **79**, 67–71.
- LEYA I., LANGE H.-J., NEUMANN S., WIELER R. AND MICHEL R. (2000) The production of cosmogenic nuclides in stony meteoroids by galactic cosmic-ray particles. *Meteorit. Planet. Sci.* **35**, 259–286.
- MASARIK J. AND REEDY R. C. (1994a) Effects of meteoroid shape on cosmogenic-nuclide production rates (abstract). *Lunar Planet. Sci.* **25**, 843–844.
- MASARIK J. AND REEDY R. C. (1994b) Effects of bulk composition on nuclide production processes in meteorites. *Geochim. Cosmochim. Acta* **58**, 5307–5317.
- MASARIK J. AND REEDY R. C. (1995) Terrestrial cosmogenic-nuclide production systematics calculated from numerical simulations. *Earth Planet. Sci. Lett.* **136**, 381–396.
- MASARIK J., CHOCHULA P. AND POVINEC P. (1992) Model for calculation of production rates of cosmogenic nuclides in extraterrestrial bodies. *J. Phys. G.: Nucl. Part. Phys.* **17**, S493–S504.
- MICHEL R., DRAGOVITSCH P., CLOTH P., DAGGE G. AND FILGES D. (1991) On the production of cosmogenic nuclides in meteoroids by galactic protons. *Meteoritics* **26**, 221–242.
- MICHEL R., LEYA I. AND BORGES L. (1996) Production of cosmogenic nuclides in meteoroids: Accelerator experiments and model calculations to decipher the cosmic ray record in extraterrestrial matter. *Nucl. Instrum. Methods Phys. Res., Sect. B* **113**, 434–444.
- MICHOLOVICH E. S., VOGT S., MASARIK J., REEDY R. C., ELMORE D. AND LIPSCHUTZ M. E. (1994) Aluminum 26,  $^{10}\text{Be}$ , and  $^{36}\text{Cl}$  depth profiles in the Canyon Diablo iron meteorite. *J. Geophys. Res.* **99**, 23 187–23 194.
- NISHIZUMI K., ARNOLD J. R., ELMORE D., FERRARO R. D., GOVE H. E., FINKEL R. C., BEUKENS R. P., CHANG K. H. AND KILIUS L. R. (1979) Measurements of  $^{36}\text{Cl}$  in Antarctic meteorites and Antarctic ice using a van de Graaff accelerator. *Earth Planet. Sci. Lett.* **45**, 285–292.
- NISHIZUMI K., REGNIER S. AND MARTI K. (1980) Cosmic ray exposure ages of chondrites, pre-irradiation and constancy of cosmic ray flux in the past. *Earth Planet. Sci. Lett.* **50**, 156–170.
- NISHIZUMI K., KLEIN J., MIDDLETON R. AND ARNOLD J. R. (1984)  $^{26}\text{Al}$  depth profile in Apollo 15 drill core. *Earth Planet. Sci. Lett.* **70**, 164–168.
- PRAEL R. E. AND LICHTENSTEIN H. (1989) *User Guide to LCS: The LAHET Code System*. Los Alamos National Laboratory Report **LA-UR-89-3014**, Natl. Tech. Info. Service, Springfield, Virginia, USA. 76 pp.
- REEDY R. C. (1985) A model for GCR-particle fluxes in stony meteorites and production rates of cosmogenic nuclides. *Proc. Lunar Planet. Sci. Conf.* **15th**, *J. Geophys. Res.* **90**, C722–C728.
- REEDY R. C. (1987) Nuclide production by primary cosmic-ray protons. *Proc. Lunar Planet. Sci. Conf.* **17th**, *J. Geophys. Res.* **92**, E697–E702.
- REEDY R. C. (1992) Solar-proton production of neon and argon (abstract). *Lunar Planet. Sci.* **23**, 1133–1134.
- REEDY R. C. AND ARNOLD J. R. (1972) Interaction of solar and galactic cosmic-ray particles with the moon. *J. Geophys. Res.* **77**, 537–555.
- REEDY R. C. AND MASARIK J. (1994) Cosmogenic-nuclide depth profiles in the lunar surface (abstract). *Lunar Planet. Sci.* **25**, 1119–1120.
- REEDY R. C., HERZOG G. F. AND JESSBERGER E. K. (1979) The reaction  $\text{Mg}(n,\alpha)\text{Ne}$  at 14.1 and 14.7 MeV: Cross sections and implications for meteorites. *Earth Planet. Sci. Lett.* **44**, 341–348.
- REEDY R. C., MASARIK J., NISHIZUMI K., ARNOLD J. R., FINKEL R. C., CAFFEE M. W., SOUTHON J., JULL A. J. T. AND DONAHUE D. J. (1993) Cosmogenic-radionuclide profiles in Knyahinya (abstract). *Lunar Planet. Sci.* **24**, 1195–1196.
- SCHULTZ L. AND KRUSE H. (1989) Helium, neon, and argon in meteorites—A data compilation. *Meteoritics* **24**, 155–172.
- VOKROUHLICKY D. AND FARINELLA P. (2000) Efficient delivery of meteorites to the Earth from a wide range of asteroid parent bodies. *Nature* **407**, 606–608.
- WASSON J. T. AND KALLEMEYN G. W. (1988) Composition of chondrites. *Phil. Trans. R. Soc. London* **A325**, 535–544.
- WELTEN K. C., NISHIZUMI K., CAFFEE M. W., MASARIK J. AND WIELER R. (2001) A complex exposure history of the Gold Basin L4-chondrite shower from cosmogenic radionuclides and noble gases (abstract). *Lunar Planet. Sci.* **32**, #2110, Lunar and Planetary Institute, Houston, Texas, USA (CD-ROM).
- WETHERILL G. W. (1980) Multiple cosmic-ray exposure ages of meteorites. *Meteoritics* **15**, 386–387.
- WETHERILL G. W. (1985) Asteroidal source of ordinary chondrites. *Meteoritics* **20**, 1–22.
- WIELER R., BAUR H., JULL A. J. T., KLANDRUD S. E., KRING D. A., LEYA I. AND MCHARGUE L. R. (2000) Cosmogenic helium, neon, and argon in the large Gold Basin chondrite (abstract). *Meteorit. Planet. Sci.* **35** (Suppl.), A169–A170.
- WRIGHT R. J., SIMMS L. A., REYNOLDS M. A. AND BOGARD D. D. (1973) Depth variation of cosmogenic noble gases in the ~120-kg Keyes chondrite. *J. Geophys. Res.* **78**, 1308–1318.